Electronic Supplementary Material (ESI) for RSC Advances.

Supplementary Information

Supporting Information for the paper entitled “Water Film inside Graphene Nanosheets: Electron Transfer Reversal between Water and Graphene via Tight Nano-confinement” by Ruixia Song, Wei Feng, Camilo A. Jimenez-Cruz, Bo Wang, Wanrun Jiang, Zhigang Wang * and Ruhong Zhou *

1. Stable conformations of GWG systems with different water densities.

2. Density distributions of hydrogen and oxygen atoms at 500 K.

3. Mulliken charge transfer of GWG system at 500 K.

4. Differential charge densities of GWG system at 300 K.

5. Electron densities of GWG system.

6. Total density of states and partial density of states at 300 K.

7. Contribution percentages of atomic orbitals to the HOMOs and the LUMOs at 300 K.

8. Total Mermin free energy of GWG system.

1. Stable conformations of GWG systems with different water densities

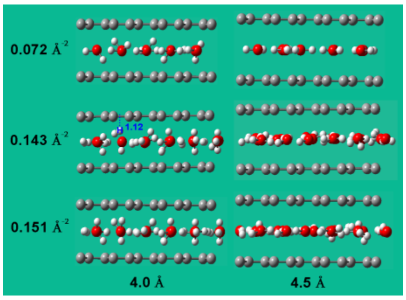

Figure S1. Stable conformations of GWG systems with water densities of 0.072 Å^{-2}, 0.143 Å^{-2} and 0.151 Å^{-2} at 4.0 and 4.5 Å, respectively.

Further structure optimization with water densities of 0.072 Å^{-2} and 0.151 Å^{-2} were performed. The stable structures are shown in Figure S1. We found that the water structures are similar for the three different water densities. That is, almost all the H atoms are parallel to the graphene sheets at the interlayer distance of 4.5 Å; however, when the distance is reduced to 4.0 Å, those H atoms not directly engaged in hydrogen bonds point perpendicularly to the graphene surface instead. This is consistent with the conclusions from the water density of 0.143 Å^{-2}.

2. Density distributions of hydrogen and oxygen atoms at 500 K

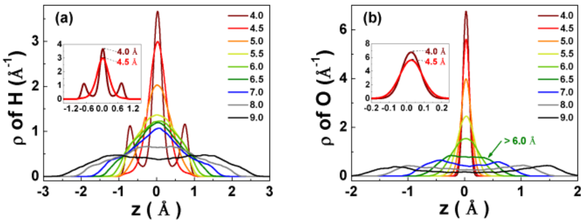

Figure S2. Density distributions of hydrogen (a) and oxygen atoms (b) of confined water molecules at 500 K, for the different interlayer distances studied.

In order to validate the conclusions of geometric relaxation and dynamical equilibrium for the systems at 300 K, we used the atomic spatial location and velocity distribution at the end of simulation at 300 K as the initial configuration, further relaxation for 100 ps at 500 K. And we analyzed density distributions of H and O atoms at 500 K in Figure S2, it can be observed that the distributional trends of H and O atoms are similar with the conclusions of 300 K. However, the dynamics of water molecules become more active at high temperature, and the distribution curves become smoother. Particularly, above d = 6.0 Å, the distribution areas of O atoms clearly become wider, and the curves tend to flatten. This phenomenon shows that the water molecules are significantly stratified, which is similar to that of 300 K. Moreover, it is notable that the density curves of H and O atoms are not completely symmetrical, especially above 6.0 Å (see arrows in Figure S2b). It can be seen that water molecules are not completely equally adsorbed in the vicinity of the graphene bilayer, but slightly inclined to one of graphene layers.

3. Mulliken charge transfer of GWG system at 500 K

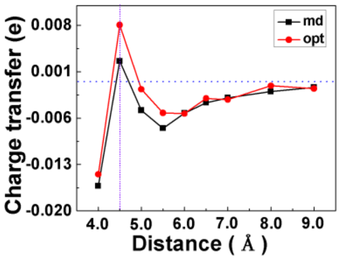

Figure S3. Mulliken charge transfer of the GWG system with different distances at 500 K, black and red represent average charge transfer in dynamic processes (md) and charge transfer of optimized structure (opt), respectively. Charge transfer value is the net charge of each water molecule. Horizontal dashed line represents 0 e.

Figure S3 shows that Mulliken charge transfer of the GWG system with different distances at 500 K, it can be seen that the trends of Mulliken charge transfer at 500 K are consistent with that of 300 K. While above 6.0 Å there is little or no charge transfer (0.000-0.005 e per water molecule), it becomes obvious when the distance is reduced to less than the vdW boundary. Particularly, for d = 4.5 Å, the water layer displays a net loss of electrons of around 0.003 e (0.008 e for optimized structure) per water molecule for dynamic processes. When the distance decreases to 4.0 Å, the electronic balance flips, and the overall water layer gains electrons in excess of 0.016 e (0.015 e for optimized structure) per water molecule for dynamic processes, which is significantly greater than the scenario of the distances above 6.0 Å.

4. Differential charge densities of GWG system at 300 K

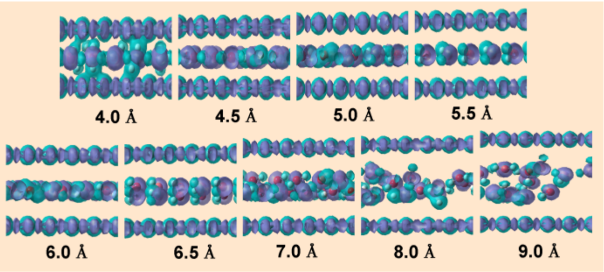

Figure S4. Differential charge densities of GWG systems with different distances at 300 K.

As shown in Figure S4, when the interlayer distances are larger than 6.0 Å, it can be seen that a small part of hydrogen atoms (non-hydrogen bonding) point to graphene bilayer, leading to the result that water molecules obtain a tiny amount of electrons, close to 0.

5. Electron densities of GWG system

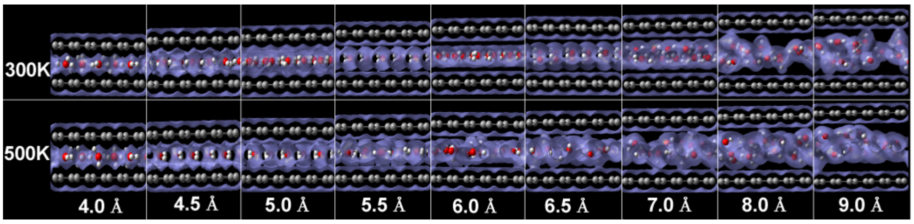

Figure S5. Electron densities of GWG systems with different distances for structural optimization, at 300 K or 500 K.

In Figure S5, it can be observed that electron densities of water molecules and upper or lower graphene layer are localized in the area around their own for the relatively large distances. And as the interlayer distances decreases, there is a phenomenon of overlapping in the electron densities of interlayer water molecules and graphene bilayer. While the interlayer distances are less than 5.5 Å, the electron densities of both the aqueous layer and the graphene bilayer are obviously overlapped.

6. Total density of states and partial density of states at 300 K

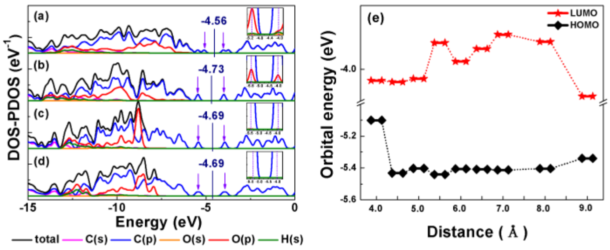

Figure S6. Total density of states (DOS) and partial density of states (PDOS) for each interlayer distance at 300 K. (a) 4.0 Å, (b) 4.5 Å, (c) 6.5 Å, (d) 9.0 Å. Inset plots detail regions near HOMO and LUMO, and their positions are marked with vertical lines. (e) Orbital energies of GWG systems with different distances at 300 K.

In order to discuss the changes of electronic structures of the GWG system with different interlayer distances, we further calculated density of states (DOS) and partial density of states (PDOS) at 4.0 Å, 4.5 Å, 6.5 Å, and 9.0 Å, respectively, as shown in Fig. S6. For the relatively large interlayer distances, the effects of distance changes on the Fermi level are only at a scale of 0.01 eV, and the graphene exhibits semiconductor properties, which are hardly changed by water doping. As the distance is reduced to 4.5 Å, 2*p* orbital contributions of O atoms to HOMO are increased, (insets in Fig. S6a and b), but OH bonds are nearly parallel to graphene sheets at d = 4.5 Å in Fig. 1, leading to small influences of water molecules on graphene, so the Fermi level shift is still small . However, compared with the previous scenario, the Fermi level at d = 4.0 Å moves to higher energy over 0.1 eV. This is due to the fact that 2*p* orbital contributions of O atoms to the HOMO are obviously more than those of the other distances (inset in Fig. S6a), leading to significantly high orbital energy of HOMO (see Supporting Information Fig. S6e), and result in the Fermi level shifting upward. The 1*s* orbital contributions of the H atoms to LUMO are observably greater than those to HOMO (green line of Fig. S6a), which again illustrates that empty 1*s* orbital of H atoms are disturbed by delocalized π orbitals formed from the *p* electrons at 4.0 Å in Fig. 3, leading to the aqueous layer capturing more electrons. Therefore, it can be seen that the Fermi levels of 4.0 Å and 4.5 Å are obviously different, since 2*p* orbital contributions of O atoms to the HOMO and the LUMO are significant changed.

7. Contribution percentages of atomic orbitals to the HOMOs and the LUMOs at 300 K

Table S1. The contribution percentages of atomic orbitals to the HOMOs and the LUMOs of GWG systems with the different distances at 300 K. Values in parentheses represent atomic orbital contributions to the LUMOs. In this work, contributions less than 0.05% for other interlayer distances are ignored.

(%)	C		O		H
	1*s*	2*p*	1*s*	2*p*	1*s*
4.0 Å	0.02 (0.00)	94.40 (98.78)	0.04 (0.02)	5.33 (0.77)	0.21 (0.43)
4.5 Å	0.01 (0.00)	97.33 (98.60)	0.03 (0.02)	2.59 (1.35)	0.04 (0.03)
5.0 Å	0.00 (0.00)	98.86 (99.42)	0.01 (0.01)	1.10 (0.55)	0.03 (0.02)

5.5 Å	0.00 (0.00)	99.66 (99.79)	0.00 (0.00)	0.33 (0.20)	0.01 (0.01)
6.0 Å	0.00 (0.00)	99.89 (99.94)	0.00 (0.00)	0.11 (0.06)	0.00 (0.00)
6.5 Å	0.00 (0.00)	99.91 (99.95)	0.00 (0.00)	0.09 (0.05)	0.00 (0.00)
7.0 Å	0.00 (0.00)	99.94 (99.97)	0.00 (0.00)	0.06 (0.03)	0.00 (0.00)
8.0 Å	0.00 (0.00)	99.95 (99.96)	0.00 (0.00)	0.05 (0.03)	0.00(0.01)
9.0 Å	0.00 (0.00)	99.97 (99.97)	0.00 (0.00)	0.03 (0.02)	0.00 (0.01)

To better describe the contributions of atomic orbitals to the HOMOs and the LUMOs at different distances, as well as the to explain the reason for almost ten-fold larger Fermi level shifting at 4.0 Å than those of other interlayer distances, we present the contribution percentages of different atomic orbitals in the system (Table S1). It could be seen that 2*p* orbital contributions of carbon atoms are greater than those of the oxygen atoms. For the relatively large distances, the contributions of the frontier orbitals are always from the 2*p* orbitals of the C atoms (more than 99%), and the effect of water doping is almost negligible. As the distance is reduced to 4.5 Å , the OH bonds are severely constrained by the graphene bilayer, but could not reach the degree of obvious invasion between 1*s* orbital of H atom and delocalized π orbitals of C atoms, therefore, H_2O molecules tend to distribute in a plane parallel to the graphene sheets as the effect of spatial confinement. Since the influence of water molecules on graphenes is small for d = 4.5 Å, there is a small shift of the Fermi level towards low energy compared with that at the large distances, presenting properties more similar to pure graphene. Interestingly, as the distance continues to decrease, at d = 4.0 Å, 2*p* orbital contributions of O atoms to the HOMO reach 5.33% (see Table S1), significantly higher than those of other interlayer distances. It is considered to be the main reason for the Fermi levels shifting in Fig. 5. Notably, 1*s* orbital of H atoms also slightly contribute to the HOMO and the LUMO about 0.21% and 0.43%, respectively. These numbers also reflect on the interactions between 1*s* orbitals of H atoms in water molecules and the delocalized π orbitals formed from *p* electrons of C atoms in graphene (we refer to it as invasion effect from H atoms to graphene). The invasion effects are well supported by the previous analysis of charge density and differential charge density (Fig. 3). And the contributions of H 1*s* orbital and O 2*p* orbital to the HOMO or the LUMO are significantly increased when d = 4.0 Å, in particular, the former is about five times larger than that of d = 4.5 Å, which closely relates with the space arrangement of OH bonds.

8. Total Mermin free energy of GWG system

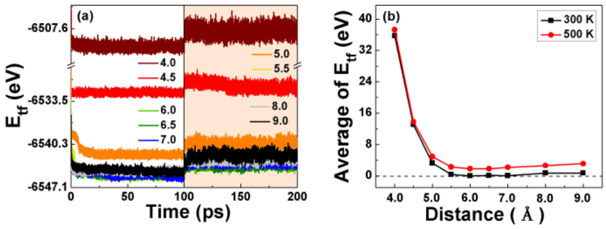

Figure S7. (a) Total Mermin free energy of system for the different interlayer distances during the dynamics simulations. 0-100 ps and 100-200 ps correspond to the energy of 300 K and 500 K, respectively. (b) Average Mermin free energy of 30-90 ps in dynamics simulation process. The free energy minimum (the distance of 6.0 Å) is used as the benchmark of 0 eV. Etf is Total Mermin free energy.

The properties of the total, time-dependent, Mermin free energy (E_{tf}) are important to address the stability of GWG, as shown in Figure S7. It can be seen that all systems reached dynamic equilibrium, and that E_{tf} decreases with the distance for the larger interlayer distances. The E_{tf} reaches a minimum at d = 6.0 Å. While, for distanced below 6.0 Å, E_{tf} increases with the distance decreases. This can be explained since, as the interlayer distance of bilayer graphene decreases, the aqueous layer becomes heavily confined. In the simulation of NVT ensemble, water molecules in interlayer display violent vibrations, forcing a high energy state in the system. Combined with Figure 1 and Figure 4, the results indicate that the relatively stable states of the GWG system are within the vicinity of d = 6.0 Å, since water molecules are entropically frustrated when the distance reduces, which leads to E_{tf} sharply increasing. Above d = 6.0 Å, there is a slight increase in the energy of GWG system, as the interlayer distance increases, because of the attraction between aqueous layer and graphene is weak.